

Detecting Spin Fractionalization in a Spinon Fermi Surface Spin Liquid: Prediction and Application for YbMgGaO₄

Yao-Dong Li¹ and Gang Chen^{1,2*}

¹State Key Laboratory of Surface Physics, Department of Physics, Center for Field Theory & Particle Physics, Fudan University, Shanghai, 200433, P.R.China and

²Collaborative Innovation Center of Advanced Microstructures, Nanjing, 210093, P.R.China

(Dated: December 3, 2024)

Continuing the recent proposal of the spinon Fermi surface U(1) spin liquid state for YbMgGaO₄ in Yao-Dong Li, *et al*, arXiv:1612.03447 and Yao Shen, *et al*, Nature 2016, we explore the experimental consequences of the external magnetic fields on this exotic state. Specifically, we focus on the *weak field regime* where the spin liquid state is preserved and the fractionalized spinon excitations remain to be a good description of the magnetic excitations. From the spin-1/2 nature of the spinon excitation, we predict the unique features of spinon continuum when the magnetic field is applied to the system. Due to the small energy scale of the rare-earth magnets, our proposal for the spectral weight shifts in the magnetic fields can be immediately tested by inelastic neutron scattering experiments. Several other experimental aspects about the spinon Fermi surface and spinon excitations are discussed and proposed. Our work provides a new way to examine the fractionalized spinon excitation and the candidate spin liquid states in the rare-earth magnets like YbMgGaO₄.

I. INTRODUCTION

A quantum spin liquid (QSL) is an exotic quantum phase of matter that carries long-range quantum entanglements and is often characterized by the emergent gauge structure and the fractionalized spin excitation¹⁻³. The experimental search of QSLs has lasted for forty years since the original proposal by Anderson in 1973^{4,5}. Many QSL candidate materials have been proposed, but the confirmation of QSLs has not been achieved in any of these materials. Recently, a rare-earth triangular lattice antiferromagnet YbMgGaO₄, that was first discovered in the power form⁶, is proposed as the first QSL candidate in the *strong spin-orbit-coupled Mott insulator* with odd electron fillings⁷⁻¹¹. This proposal is compatible with the more fundamental view based on the time reversal symmetry and quantum entanglements^{7-9,11,12}. Due to the unprecedented experimental advantage such as the availability of large high-quality single-crystal samples⁷, YbMgGaO₄ may stand out as another important QSL candidate for which a variety of experimental techniques can be implemented and the theoretical proposal and ideas may be directly tested.

The Yb local moments in YbMgGaO₄ remain disordered down to the lowest measured temperature at which the magnetic entropy is almost exhausted^{6,9,13,14}. The low-temperature heat capacity has a sub-linear temperature dependence^{6,14,15} that is close to the $C_v \propto T^{2/3}$ behavior for the spinon Fermi surface U(1) QSL¹⁶⁻¹⁸. More substantially, the dynamic spin structure, that is measured by the inelastic neutron scattering on single-crystal samples^{9,14}, shows a reasonable agreement with the theoretical prediction for the spinon Fermi surface state^{9,11,16-18}.

There are two major questions concerning the candidate QSL state in YbMgGaO₄. The first and probably *the most crucial one* is whether the excitation continuum

from the inelastic neutron scattering is truly a spinon continuum and represents the spin quantum number fractionalization. The second question is the microscopic mechanism for the QSL behavior of YbMgGaO₄. It was suggested that the anisotropic interaction of the local moments, due to the spin-orbit entanglement, could enhance the quantum fluctuation and destabilize the magnetically ordered phases^{7,8,10}. This observation was first proposed as one possible mechanism for the QSL behavior in YbMgGaO₄^{7,8}, and explained in details in Refs. 8 and 10. Both questions have been partially addressed by the mean-field theory analysis⁹ and the later projective symmetry analysis^{9,11} that identify the spinon Fermi surface U(1) QSL as the candidate ground state for YbMgGaO₄. Clearly, this exotic state provides a consistent explanation for both thermodynamic and spectroscopic behaviors of YbMgGaO₄⁹.

Ideally, it would be nice to directly solve our microscopic spin model and see if one can obtain any QSL ground state in the phase diagram, then both questions may be completely resolved. Due to the complication of the model, this is difficult even numerically^{8,11}. In this work, instead of directly tackling the anisotropic spin model^{8,10,19}, we work on the spinon mean-field Hamiltonian^{9,11} and address the first question about *how to detect or confirm the very existence of the fractionalized spinon excitations* in YbMgGaO₄. We propose a simple experimental scheme to test the spin quantum number fractionalization and confirm the spinon excitation. We suggest to apply a *weak external magnetic field* and study the spectral weight shifts of the dynamic spin structure factor. The splitting of the degenerate spinon bands by the magnetic field is directly revealed by the spinon particle-hole continuum that is detected by the dynamic spin structure factor. We show that the persistence of the spinon continuum, the spectral weight shifts and the spectral crossing around the Γ point, the existence of the

upper and lower excitation edges under the weak magnetic field represent unique properties of the spinon excitation for the spinon Fermi surface state, and thus provide a sharp experimental prediction for the identification of the spinon excitation with respect to the spinon Fermi surface.

The remaining part of the paper is organized as follows. In Sec. II, we explain our view on the magnetic excitation continuum and the weak spectral weight in the inelastic neutron scattering results on YbMgGaO₄ and motivate our approach in this paper. In Sec. III, we justify the mean-field Hamiltonian in the magnetic field. In Sec. IV, we obtain the dynamic spin structure factor from the free spinon theory in the magnetic field and explain the spectral weight shifts. In Sec. V, we repeat the calculation in Sec. IV with a RPA calculation that includes the spinon interactions. Finally in Sec. VI, we conclude with a discussion about various future experimental direction for the spinon Fermi surface state.

II. THE SPINON FERMI SURFACE STATE

We start with the fermionic parton construction for the spin operator with $\mathbf{S}_i = \frac{1}{2}f_{i\alpha}^\dagger \boldsymbol{\sigma}_{\alpha\beta} f_{i\beta}$, where $f_{i\alpha}^\dagger$ ($f_{i\alpha}$) creates (annihilates) one spinon with spin α ($=\uparrow, \downarrow$) at the site i and $\boldsymbol{\sigma} = (\sigma^x, \sigma^y, \sigma^z)$ is a vector of Pauli matrices. This construction is further supplemented by a Hilbert space constraint $\sum_\alpha f_{i\alpha}^\dagger f_{i\alpha} = 1$. At the mean-field level, the following spinon Hamiltonian,

$$H_{\text{MF}} = -t_1 \sum_{\langle ij \rangle, \alpha} f_{i\alpha}^\dagger f_{j\alpha} - t_2 \sum_{\langle\langle ij \rangle\rangle, \alpha} f_{i\alpha}^\dagger f_{j\alpha} - \mu \sum_{i, \alpha} f_{i\alpha}^\dagger f_{i\alpha} \quad (1)$$

was proposed for YbMgGaO₄ and gives a large spinon Fermi surface^{9,11}. Here the chemical potential μ is introduced to impose the Hilbert space constraint. It was found that the spinon particle-hole excitation of this simple state provides a consistent magnetic excitation continuum with the inelastic neutron scattering experiments. Moreover, the anisotropic spin interaction, that is included into the the spinon mean-field theory by a random phase approximation (RPA), gives a weak spectral peak at the M points, which is also consistent with the experimental observation.

The spinon continuum is much more important than the weak spectral peak. The spectral peak at certain momenta merely represents some collective mode of the spinons that is enhanced by the residual and short-range interaction between the fermionic spinons, and is quite common for example in the Fermi liquids of electrons as an analogy. Nevertheless, the spectral peak does provide hints about the form of the microscopic interactions. In contrast, the spinon continuum is a consequence of the spin quantum number fractionalization that reveals the defining nature of QSLs.

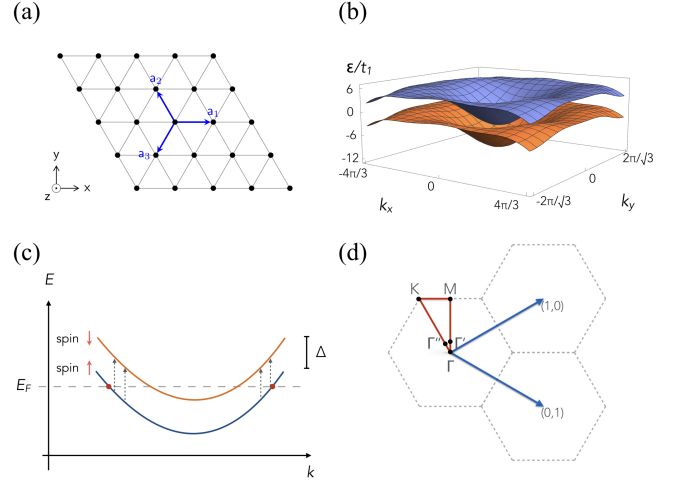


FIG. 1. (Color online.) (a) The Yb triangular lattice with $\mathbf{a}_1, \mathbf{a}_2, \mathbf{a}_3$ bonds. (b) The spinon band structure for $\Delta = 0.6B$ and $t_2/t_1 = 0.2$ (this value is optimized for the variational energy; see main text). (c) A schematic illustration of the spinon band structure and the particle-hole excitation for the zero momentum transfer. (d) The Brillouin zone of the triangular lattice, with high-symmetry points and the basis vectors (in r.l.u. coordinates) highlighted.

Since we think the spinon continuum is more important and the spinon continuum is already obtained by the free-spinon theory of H_{MF} , our approach will mostly rely on the free-spinon mean-field theory and focus more on the spinon continuum rather than the weak spectral peak. The (short-range) anisotropic spin interaction will be included into the free-spinon theory in the later parts of the paper. The coupling to the gapless U(1) gauge photon is not included through this paper. This spin-gauge coupling has an important effect on the low-energy properties of the system^{16,17}.

III. COUPLING TO THE MAGNETIC FIELD

Unlike the electron, the fermionic spinon is a charge neutral object and does not couple to the external magnetic field via the Lorentz coupling. Here, we point out that the prior theory on the organic spin liquid material²⁰ $\kappa\text{-(ET)}_2\text{Cu}_2(\text{CN})_3$ has actually invoked the interesting Lorentz coupling of the spinons to the external magnetic field *indirectly* through the internal U(1) gauge flux²¹. This is because the the organic material $\kappa\text{-(ET)}_2\text{Cu}_2(\text{CN})_3$ is in the weak Mott regime where the charge gap is small and the four-spin ring exchange interaction can be significant¹⁸. It is the four-spin ring exchange that connects and transfers the external magnetic flux to the internal emergent U(1) gauge flux²¹. In contrast, the $4f$ electrons of the Yb ions are in the *strong Mott regime* and is very localized. As we have explained, the effective spin \mathbf{S}_i arises from the strong spin-orbit coupling (SOC) and crystal electric field splitting,

and the four-spin ring exchange is strongly suppressed due to the very large on-site interaction of the 4f electrons. Therefore, the orbital coupling to the magnetic field of the spinons in the organic spin liquid does not apply to YbMgGaO₄. Although the strong magnetic field fully polarizes the Yb local moments along the field direction and thus destabilizes the spin liquid state, in the weak field regime, the field does not change the spin liquid ground state and the spinon remains to be a valid description of the magnetic excitation. From the above argument, if YbMgGaO₄ ground state is a spinon Fermi surface QSL, the appropriate spinon mean-field Hamiltonian for YbMgGaO₄ in a weak external magnetic field should be

$$H_{\text{MFh}} = -t_1 \sum_{\langle ij \rangle, \alpha} f_{i\alpha}^\dagger f_{j\alpha} - t_2 \sum_{\langle\langle ij \rangle\rangle, \alpha} f_{i\alpha}^\dagger f_{j\alpha} - \sum_{i, \alpha\beta} g_z \mu_B h_z f_{i\alpha}^\dagger \frac{\sigma_{\alpha\beta}^z}{2} f_{i\beta} - \mu \sum_{i, \alpha} f_{i\alpha}^\dagger f_{i\alpha}, \quad (2)$$

where only Zeeman coupling is needed, and g_z is the Landé factors for the field normal to the triangular plane, respectively. The mean-field Hamiltonian in Eq. (2) will be the basis of the analysis below.

IV. SPECTRAL WEIGHT SHIFTS FROM THE FREE-SPINON THEORY

For each magnetic field, the spinon hopping and the chemical potential in Eq. (2) need to be re-determined by optimizing the variational energy of the microscopic spin Hamiltonian $H_{\text{Spin-h}}$ that is

$$H_{\text{Spin-h}} = \sum_{\langle ij \rangle} [J_{zz} S_i^z S_j^z + J_{\pm} (S_i^+ S_j^- + S_i^- S_j^+)] + J_{\pm\pm} (\gamma_{ij} S_i^+ S_j^+ + \gamma_{ij}^* S_i^- S_j^-) - \frac{\mathbb{J}_{z\pm}}{2} ((\gamma_{ij}^* S_i^+ - \gamma_{ij} S_i^-) S_j^z + \langle i \leftrightarrow j \rangle)] - \sum_i g_z \mu_B h_z S_i^z. \quad (3)$$

Here γ_{ij} 's are the bond-dependent phase variables that arises from the spin-orbit coupling of the Yb 4f electrons^{7,8,10,11}, and $\gamma_{ij} = 1, e^{i2\pi/3}, e^{-i2\pi/3}$ for ij along the $\mathbf{a}_1, \mathbf{a}_2, \mathbf{a}_3$ bond, respectively. Throughout the paper, we set $J_{\pm} = 0.915 J_{zz}$. The z -direction magnetic field shifts the chemical potential for the spin- \uparrow and spin- \downarrow spinons up and down such that the spinon excitations are given by

$$\xi_{\uparrow}(\mathbf{k}) = \epsilon(\mathbf{k}) - \mu_{\uparrow} \equiv \epsilon(\mathbf{k}) - (\mu + \frac{g_z \mu_B h_z}{2}), \quad (4)$$

$$\xi_{\downarrow}(\mathbf{k}) = \epsilon(\mathbf{k}) - \mu_{\downarrow} \equiv \epsilon(\mathbf{k}) - (\mu - \frac{g_z \mu_B h_z}{2}), \quad (5)$$

where $\epsilon(\mathbf{k})$ is the dispersion that is obtained from the first line of Eq. (2). In Fig. 1, we plot the mean-field

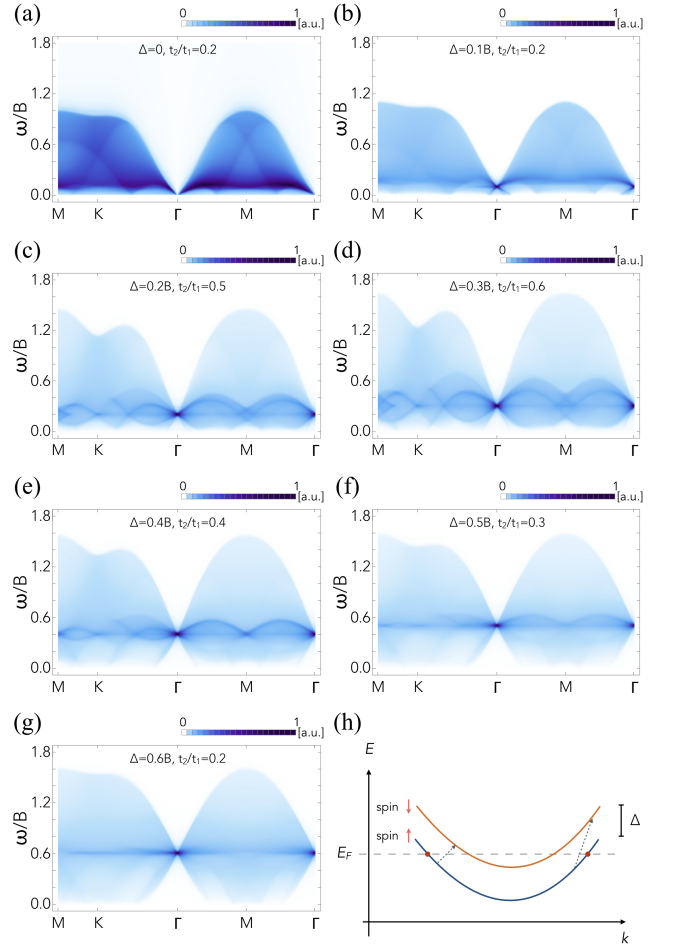


FIG. 2. (a-g) Dynamic spin structure factors for free spinon theory with z -direction magnetic field up to $0.6B$, where $B = 9.6t_1$ is the bandwidth for the free spinon theory without the field in Eq. (1). The values of t_2/t_1 are optimized from the variational energy. (h) Illustration of the particle-hole excitations with small momenta. Such excitations for each \mathbf{q} are degenerate at zero field, and the 2-fold degeneracy is lifted as soon as the field is turned on.

dispersions of the spinons in the magnetic field, where the spin up and spin down spinons have different Fermi surfaces. Therefore, in the weak field regime, the system remains gapless.

In the inelastic neutron scattering measurement, the neutron spin flip excites the spinon particle-hole pairs across the spinon Fermi surface. In the free-spinon theory, the energy and momentum change of the neutron, ω and \mathbf{p} , is shared by the one spinon particle-hole pair, and we have

$$\mathbf{p} = \mathbf{k}_1 - \mathbf{k}_2, \quad (6)$$

$$\omega(\mathbf{p}) = \xi_{\downarrow}(\mathbf{k}_1) - \xi_{\uparrow}(\mathbf{k}_2). \quad (7)$$

In the mean-field theory, the field essentially breaks the degenerate spinon bands by separating the dispersions of spin- \uparrow and spin- \downarrow spinon bands in energy with a Zeeman splitting. Thus, there exists a large density of particle-

hole excitations at the zero momentum transfer with the energy $\omega(\mathbf{0}) = g_z \mu_B h_z \equiv \Delta$ (see the illustration in Fig. 1b). We thus expect a spectral peak at the Γ point with a finite energy transfer Δ . Without the magnetic field, we have shown in Refs. 9 and 11 that the spectral weight at the finite energy is suppressed at the Γ point.

In Fig. 2, we calculate the dynamic spin structure factor $\mathcal{S}(\mathbf{q}, \omega)$ for various values of the magnetic field h_z on a lattice of size 200×200 . Here $\mathcal{S}(\mathbf{q}, \omega)$ is given by

$$\mathcal{S}(\mathbf{q}, \omega) = \frac{1}{N} \sum_{i,j} e^{i\mathbf{q} \cdot (\mathbf{r}_i - \mathbf{r}_j)} \int dt e^{-i\omega t} \langle S_{\mathbf{r}_i}^-(t) S_{\mathbf{r}_j}^+(0) \rangle \quad (8)$$

where N is the system size and the expectation is taken with respect to the spinon Fermi surface ground state of the mean-field Hamiltonian. In the above equation, the time integration yields a delta function for the energy conservation, and we replace the delta function by $\delta(\omega) = \frac{\eta/\pi}{\omega^2 + \eta^2}$ with $\eta = 0.1t_1$ in the following calculation. First we observe that the spectrum *remains gapless* at the weak field regime. Second, we indeed find that the spectral weight at the Γ point occurs at the energy transfer Δ due to the structure of the spinon bands that were discussed previously.

Apart from the enhancement of the spectral intensity at the Γ point and the Zeeman splitting energy, there is an interesting spectral crossing near the Zeeman splitting energy Δ around the Γ point. This is one important consequence of the external magnetic field on the spinon continuum. To understand this phenomenon, we start from the vertical particle-hole transition in Fig. 1b and slightly tilt the transition such that the momentum transfer of the neutron is finite but small (see Fig. 2h). Depending on the tilting direction of the momentum, the energy transfer can be greater or smaller than Δ and take the value $\Delta \pm \mathbf{v} \cdot \mathbf{q}$, where we have linearized the dispersion and $\mathbf{v} \approx \mathbf{v}_F$ in the weak field limit. In principle, the velocity \mathbf{v} would depend on the momenta of the spinon particle and spinon hole, but for the convenience of presentation, such dependence is not indicated. The neutron energy transfer is thus located within the energy range $(\Delta - vq, \Delta + vq)$, and this explains the upper and lower excitation edges near the Γ point.

The above behaviors of spinon continuum in the weak magnetic field are *qualitatively* different from what one would expect for the magnon-like excitation. For the magnons that are integer-spin excitations, the magnetic field directly couples to the magnon, most often shifts the whole magnon band by gapping out the low-energy modes. The magnon lifetime becomes longer, the magnon quasi-particle become sharper, and the magnon band would be narrowed. In contrast, for the spinons that are spin-1/2 excitations, the magnetic field shifts the spin-up spinon and the spin-down spinon bands oppositely. The spinon continuum in the magnetic field is sensitive to the dispersions of both spinon bands and thus reflects the fractionalized nature of the magnetic excitations. It is hard to imagine the *broad excitation continuum*, the *spectral crossing* at Γ and $\omega = \Delta$, and the *upper*

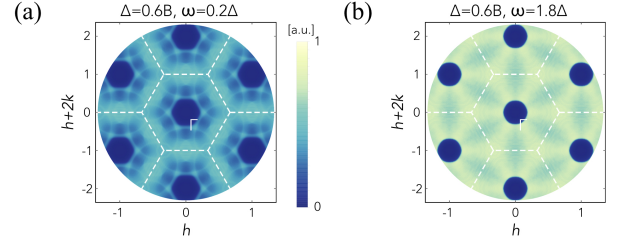


FIG. 3. Momentum resolved dynamic spin structure factor at the energy cuts above and below the Zeeman splitting Δ . (a) and (b) share the same intensity bar. For both plots, the spectral weights in the region near the Γ point are suppressed.

and lower excitation edges near the Γ point in Fig. 2 can be obtained from the magnon-like excitation under the magnetic field.

Another feature of the spinon continuum in the weak magnetic field is the suppression of the overall intensity. Originally at the zero field, the spectral weight is suppressed above an upper excitation edge (see Fig. 2a). The weak magnetic fields create spectral weights near the Γ point at finite energies, i.e. in the regions where the spectral weights are suppressed at zero field. Therefore, the overall intensity of the continuum is suppressed at the small magnetic field.

To further manifest two excitation edges near the Γ point and $\omega = \Delta$, we depict the dynamic spin structure factor in the Brillouin zone for different neutron energy transfers in Fig. 3. The intensity distribution within the Brillouin zone further reflects the variation of the spinon band structure under the magnetic field. For the energy and the momentum below the lower excitation edge in Fig. 2, the spectral weight is strongly suppressed, leading to a reduced spectral intensity around the Γ points (see Fig. 3a). Likewise, for the energy above the upper excitation edge in Fig. 2, the spectral intensity around the Γ points is similarly suppressed (see Fig. 3b). Nevertheless, for energy right at Δ , the spectral intensity around the Γ points is not suppressed due to the reason that was explained previously.

The energy distribution curve (EDC) of $\mathcal{S}(\mathbf{q}, \omega)$ at certain momenta is a common measurement with inelastic neutron scattering that could reveal important information of the ground state. We depict the EDC in Fig. 4. The peak at the Γ point and the shift of the peak position under the magnetic field are the most salient experimental features, and can be readily probed using inelastic neutron scattering and/or optical measurements. Off the Γ point, the spectral peak in the EDC becomes broad since the finite momentum transfer allows a range of energies for the spinon particle-hole continuum, and the energy range of the peak is bounded by the upper and lower excitation edges.

Finally, we comment on the caveat of the mean-field theory. In the mean-field theory for the spinons, we have ignored the spinon-gauge coupling. The gapless U(1) gauge photon is expected to play an important role at

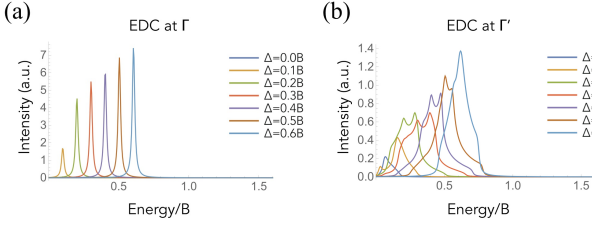


FIG. 4. Energy-dependent curves of the dynamic spin structure factor at (a) Γ and (b) Γ' (see Fig. 1d). Right at Γ , there is a narrow Zeeman peak for nonzero fields whose position shifts with the field. Away from Γ , there is a broad continuum corresponding to the spinon particle-hole excitations. Note that the very low-energy part of spectral weight is underestimated in the mean-field theory due to the neglecting of the gauge fluctuation.

low energies. For example, the Yukawa coupling between the fermionic spinons and the gapless U(1) gauge photon would give rise a self-energy correction to the spinon Green's function and thus enhance the low-energy density of states^{16,17}. Therefore, the inelastic neutron scattering process that excites the spinon particle-hole pair, would have an enhanced spectral weight at low energies. This property is not captured in the spinon mean-field theory. We thus expect the very low energy spectral weights in Figs. 2,4 and also in Fig. 5 to be enhanced when the gauge fluctuation is included. Moreover, the slight enhancement of the overall bandwidth of the spinon continuum in the field is probably a mean-field artifact as well because the bandwidth should be set by the exchange interaction of the system.

V. THE RPA CORRECTION FROM THE ANISOTROPIC INTERACTION

As we have proposed in Ref. 8, the anisotropic spin exchange terms $J_{\pm\pm}$ and $J_{z\pm}$ from the strong SOC in Eq. (3) is likely to play an important role in stabilizing the QSL ground state. The SOC is further suggested to be responsible for the weak spectral peak at the M point^{9–11}. Here we consider the effect of the anisotropic spin interaction on the dynamic spin structure factors following a phenomenological approach introduced in Refs. 11 and 22. Starting from the free-spinon theory H_{MFh} and the corresponding susceptibility $\chi^0(\mathbf{q}, \omega)$, we treat the anisotropic interaction H'_{spin} as perturbations. The resulting magnetic susceptibility is calculated in the random phase approximation (RPA)²²,

$$\chi^{\text{RPA}}(\mathbf{q}, \omega) = [\mathbf{1} - \chi^0(\mathbf{q}, \omega) \mathcal{J}(\mathbf{q})]^{-1} \chi^0(\mathbf{q}, \omega), \quad (9)$$

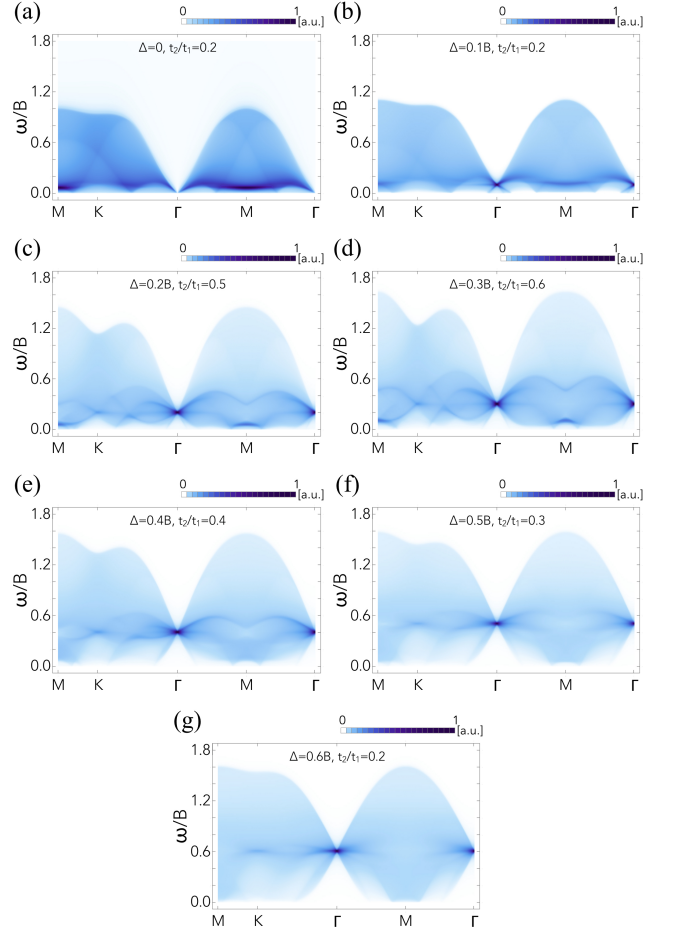


FIG. 5. Dynamic spin structure factors for the interacting spinon theory with external magnetic field along z -direction up to $0.6B$, where the interaction is given by H'_{Spin} .

where $\mathcal{J}(\mathbf{q})$ is the exchange matrix from H'_{spin} ,

$$\mathcal{J}(\mathbf{q}) = \begin{pmatrix} 2(u_{\mathbf{q}} - v_{\mathbf{q}}) J_{\pm\pm} & -2\sqrt{3}w_{\mathbf{q}} J_{\pm\pm} & -\sqrt{3}w_{\mathbf{q}} J_{z\pm} \\ -2\sqrt{3}w_{\mathbf{q}} J_{\pm\pm} & 2(v_{\mathbf{q}} - u_{\mathbf{q}}) J_{\pm\pm} & (u_{\mathbf{q}} - v_{\mathbf{q}}) J_{z\pm} \\ -\sqrt{3}w_{\mathbf{q}} J_{z\pm} & (u_{\mathbf{q}} - v_{\mathbf{q}}) J_{z\pm} & 0 \end{pmatrix} \quad (10)$$

with $u_{\mathbf{q}} = \cos(\mathbf{q} \cdot \mathbf{a}_1)$, $v_{\mathbf{q}} = \frac{1}{2}[\cos(\mathbf{q} \cdot \mathbf{a}_2) + \cos(\mathbf{q} \cdot \mathbf{a}_3)]$, and $w_{\mathbf{q}} = \frac{1}{2}[\cos(\mathbf{q} \cdot \mathbf{a}_2) - \cos(\mathbf{q} \cdot \mathbf{a}_3)]$.

The RPA corrected dynamic spin structure factor is related $\chi^{\text{RPA}}(\mathbf{q}, \omega)$ by the equation $\mathcal{S}^{\text{RPA}}(\mathbf{q}, \omega) = -\frac{1}{\pi} \text{Im}[\chi^{\text{RPA}}(\mathbf{q}, \omega)]^{+-}$. The renormalized dynamic spin structure factor $\mathcal{S}^{\text{RPA}}(\mathbf{q}, \omega)$ is shown in the Fig. 5, where we choose the parameters to be $J_{z\pm}/t_1 = 0.2$, $J_{\pm\pm}/t_1 = 0.35$. From the results we conclude that the anisotropic exchange terms merely redistribute the spectral weight within the Brillouin zone and leave the qualitative features in the vicinity of the Γ point mentioned in previous sections unaffected.

VI. DISCUSSION

Our prediction of *the qualitative behaviors* of the spinon continuum in the magnetic field relies on the spinon mean-field theory and the proposed spin liquid ground state. The microscopic spin model does not play a significant role in our experimental prediction, but the feasibility of the experiments in the magnetic field strongly relies on the fact that the microscopic interactions between the Yb local moments in YbMgGaO_4 are of the order of a couple Kelvins⁷. The magnetic field in the laboratory could readily lead to a visible effect on the spinon continuum. In contrast, the exchange couplings of other spin liquid candidate materials such as the organics^{20,23,24} and herbertsmithite^{25,26} are of the order of 100K, and a much larger field is required there.

The previous works^{14,27} (including our earlier theoretical work^{8,10}) have explored the strong field regime, where the magnetic excitations are simply the *gapped* magnons with respect to an almost fully polarized state along the field directions. These works may provide useful information about the spin interaction, but do not give information about the spin quantum number fractionalization since the ground state is no longer a spin liquid state. The *weak field* regime, that is proposed in this work, directly accesses the spin liquid phase. Our predictions of the (gapless) spinon continuum, the spectral weight shifts, the spectral crossing, and the upper and lower excitation edges in the weak magnetic field directly reveal the fractionalized spinon excitations. If these predictions are confirmed, it will give a strong support of the spinon Fermi surface spin liquid ground state in YbMgGaO_4 .

Apart from the fractionalization, the emergence of the Fermi statistics for the spinons is a rather unusual phenomenon. Although the particular structure of the

spinon continuum is a direct consequence of the spinon Fermi surface and the spinon Fermi statistics, directly confirming the Fermi statistics is certainly desirable. The temperature dependence of the dynamic spin structure factor could provide hints for the Fermi statistics. Moreover, the spin-orbital-entangled nature of the Yb local moments may provide a route to visualize the spinon Fermi surface. Clearly, the orbital degrees of freedom are sensitive to the ion position. The Yb local moment, that results from the spin-orbital entanglement, may be more susceptible to the lattice degrees of freedom than the conventional spin-only moment. Therefore, like the electron-phonon coupling in Fermi liquids, one may expect a similar “ $2k_F$ ” Kohn anomaly²⁸ in the phonon spectrum that arises from the spinon-phonon coupling in YbMgGaO_4 and use the Kohn anomaly to construct the spinon Fermi surface.

Finally, as we have already pointed out in Ref. 11, the phase transition from the candidate QSL ground state in the weak field regime to the fully polarized state in the strong field regime is an interesting open question that needs further theoretical and experimental investigation. Experimentally, it is feasible to study the nature of this transition in YbMgGaO_4 with fine field variations.

VII. ACKNOWLEDGEMENTS

This work is supported by the Ministry of Science and Technology of People’s Republic of China with the Grant No.2016YFA0301001 (G.C.), the Start-Up Funds and the Program of First-Class University Construction of Fudan University (G.C.), and the Thousand-Youth-Talent Program (G.C.) of People’s Republic of China. G.C. thanks the hospitality of Prof Ying Ran at Boston College during the visit in January 2017 when this work is finalized.

* gangchen.physics@gmail.com

¹ Leon Balents, “Spin liquids in frustrated magnets,” *Nature* **464**, 199–208 (2010).

² Lucile Savary and Leon Balents, “Quantum spin liquids,” arXiv preprint arXiv:1601.03742 (2016).

³ Patrick A. Lee, “An end to the drought of quantum spin liquids,” *Science* **321**, 1306–1307 (2008).

⁴ P.W. Anderson, “Resonating valence bonds: A new kind of insulator?” *Materials Research Bulletin* **8**, 153–160 (1973).

⁵ P.W. Anderson, “The Resonating Valence Bond State in La_2CuO_4 and Superconductivity,” *Science* **235**, 1196–1198 (1987).

⁶ Yuesheng Li, Haijun Liao, Zhen Zhang, Shiyun Li, Feng Jin, Langsheng Ling, Lei Zhang, Youming Zou, Li Pi, Zhaorong Yang, Junfeng Wang, Zhonghua Wu, and Qingming Zhang, “Gapless quantum spin liquid ground state in the two-dimensional spin-1/2 triangular antiferromagnet YbMgGaO_4 ,” *Scientific Reports* **5**, 16419 (2015).

⁷ Yuesheng Li, Gang Chen, Wei Tong, Li Pi, Juanjuan Liu, Zhaorong Yang, Xiaoqun Wang, and Qingming Zhang,

“Rare-Earth Triangular Lattice Spin Liquid: A Single-Crystal Study of YbMgGaO_4 ,” *Phys. Rev. Lett.* **115**, 167203 (2015).

⁸ Yao-Dong Li, Xiaoqun Wang, and Gang Chen, “Anisotropic spin model of strong spin-orbit-coupled triangular antiferromagnets,” *Phys. Rev. B* **94**, 035107 (2016).

⁹ Yao Shen, Yao-Dong Li, Hongliang Wo, Yuesheng Li, Shoudong Shen, Bingying Pan, Qisi Wang, H. C. Walker, P. Steffens, M Boehm, Yiqing Hao, D. L. Quintero-Castro, L. W. Harriger, Lijie Hao, Siqin Meng, Qingming Zhang, Gang Chen, and Jun Zhao, “Spinon Fermi surface in a triangular lattice quantum spin liquid YbMgGaO_4 ,” *Nature*, arXiv preprint 1607.02615 (2016), 10.1038/nature20614.

¹⁰ Yao-Dong Li, Yao Shen, Yuesheng Li, Jun Zhao, and Gang Chen, “The effect of spin-orbit coupling on the effective-spin correlation in YbMgGaO_4 ,” arXiv preprint 1608.06445 (2016).

¹¹ Yao-Dong Li, Yuan-Ming Lu, and Gang Chen, “The Spinon Fermi Surface U(1) Spin Liquid in a Spin-Orbit-Coupled Triangular Lattice Mott Insulator YbMgGaO_4 ,”

- arXiv preprint 1612.03447 (2016).
- ¹² Haruki Watanabe, Hoi Chun Po, Ashvin Vishwanath, and Michael Zaletel, “Filling constraints for spin-orbit coupled insulators in symmorphic and nonsymmorphic crystals,” *PNAS* **112**, 14551–14556 (2015).
 - ¹³ Yuesheng Li, Devashibhai Adroja, Pabitra K. Biswas, Peter J. Baker, Qian Zhang, Juanjuan Liu, Alexander A. Tsirlin, Philipp Gegenwart, and Qingming Zhang, “Muon Spin Relaxation Evidence for the U(1) Quantum Spin-Liquid Ground State in the Triangular Antiferromagnet YbMgGaO₄,” *Phys. Rev. Lett.* **117**, 097201 (2016).
 - ¹⁴ Joseph A. M. Paddison, Zhiling Dun, Georg Ehlers, Yao-hua Liu, Matthew B. Stone, Haidong Zhou, and Martin Mourigal, “Continuous excitations of the triangular-lattice quantum spin liquid YbMgGaO₄,” *Nature Physics*, arXiv preprint 1607.03231 (2016).
 - ¹⁵ Y. Xu, J. Zhang, Y. S. Li, Y. J. Yu, X. C. Hong, Q. M. Zhang, and S. Y. Li, “Absence of Magnetic Thermal Conductivity in the Quantum Spin-Liquid Candidate YbMgGaO₄,” *Phys. Rev. Lett.* **117**, 267202 (2016).
 - ¹⁶ Patrick A. Lee and Naoto Nagaosa, “Gauge theory of the normal state of high- T_c superconductors,” *Phys. Rev. B* **46**, 5621–5639 (1992).
 - ¹⁷ Sung-Sik Lee and Patrick A. Lee, “U(1) Gauge Theory of the Hubbard Model: Spin Liquid States and Possible Application to κ -(BEDT-TTF)₂Cu₂(CN)₃,” *Phys. Rev. Lett.* **95**, 036403 (2005).
 - ¹⁸ Olexei I. Motrunich, “Variational study of triangular lattice spin-1/2 model with ring exchanges and spin liquid state in κ -(ET)₂Cu₂(CN)₃,” *Phys. Rev. B* **72**, 045105 (2005).
 - ¹⁹ Changle Liu, Rong Yu, and Xiaoqun Wang, “Semiclassical ground-state phase diagram and multi- q phase of a spin-orbit-coupled model on triangular lattice,” *Phys. Rev. B* **94**, 174424 (2016).
 - ²⁰ Y. Shimizu, K. Miyagawa, K. Kanoda, M. Maesato, and G. Saito, “Spin liquid state in an organic mott insulator with a triangular lattice,” *Phys. Rev. Lett.* **91**, 107001 (2003).
 - ²¹ Olexei I. Motrunich, “Orbital magnetic field effects in spin liquid with spinon fermi sea: Possible application to κ -(ET)₂Cu₂(CN)₃,” *Phys. Rev. B* **73**, 155115 (2006).
 - ²² Jan Brinckmann and Patrick A. Lee, “Slave Boson Approach to Neutron Scattering in YBa₂Cu₃O_{6+y} Superconductors,” *Phys. Rev. Lett.* **82**, 2915–2918 (1999).
 - ²³ T. Itou, A. Oyamada, S. Maegawa, M. Tamura, and R. Kato, “Quantum spin liquid in the spin-1/2 triangular antiferromagnet EtMe₃Sb[Pd(dmit)₂]₂,” *Phys. Rev. B* **77**, 104413 (2008).
 - ²⁴ T Itou, A Oyamada, S Maegawa, M Tamura, and R Kato, “Spin-liquid state in an organic spin-1/2 system on a triangular lattice, EtMe₃Sb[Pd(dmit)₂]₂,” *Journal of Physics: Condensed Matter* **19**, 145247 (2007).
 - ²⁵ Tian-Heng Han, Joel S Helton, Shaoyan Chu, Daniel G Nocera, Jose A Rodriguez-Rivera, Collin Broholm, and Young S Lee, “Fractionalized excitations in the spin-liquid state of a kagome-lattice antiferromagnet,” *Nature* **492**, 406–410 (2012).
 - ²⁶ P. Mendels, F. Bert, M. A. de Vries, A. Olariu, A. Harrison, F. Duc, J. C. Trombe, J. S. Lord, A. Amato, and C. Baines, “Quantum magnetism in the paratacamite family: Towards an ideal kagomé lattice,” *Phys. Rev. Lett.* **98**, 077204 (2007).
 - ²⁷ Yuesheng Li, Devashibhai Adroja, Robert I. Bewley, David Voneshen, Alexander A. Tsirlin, Philipp Gegenwart, and Qingming Zhang, “Crystalline Electric Field Randomness in the Triangular Lattice Spin-Liquid YbMgGaO₄,” arXiv preprint arXiv:1702.01981 (2017).
 - ²⁸ David F. Mross and T. Senthil, “Charge Friedel oscillations in a Mott insulator,” *Phys. Rev. B* **84**, 041102 (2011).